Simulation of Photoluminescence Spectra

Speaker: Yu Jin

MICCoM Workshop

10/14/2022

Introduction

Motivation: Materials characterization requires the ability to simulate **photoluminescence (PL) spectra**

Light emitting all inorganic perovskites

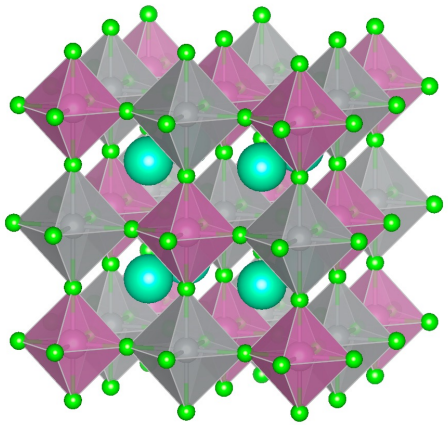

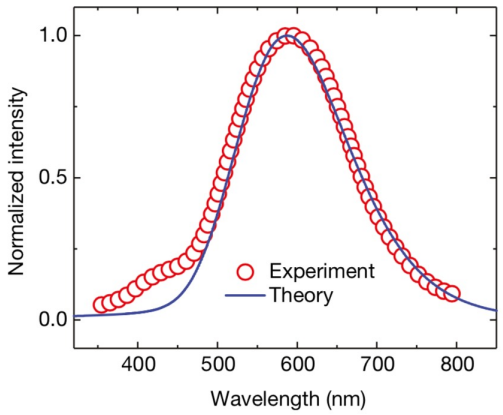

e.g., All inorganic perovskite $Cs_2AgInCl_6$

J. Luo et al., *Nature*. **563**, 541 (2018).

Defect systems for quantum information science

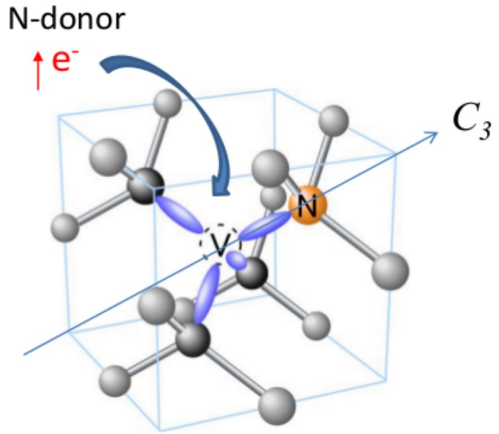

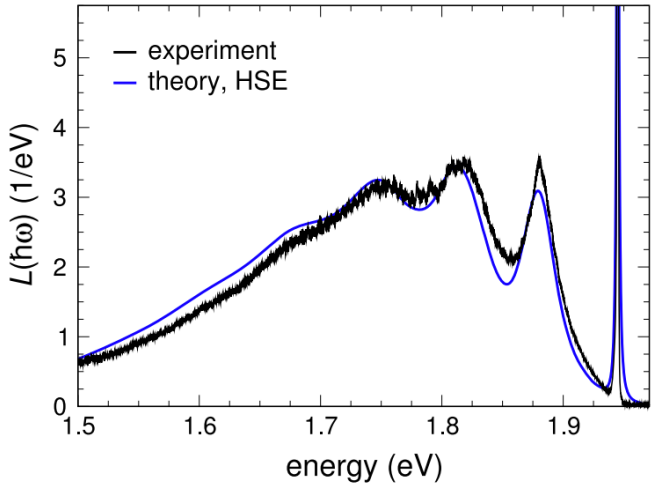

e.g., NV^- center in diamond

A. Alkauskas et al., *New J. Phys*. **24**, 073026 (2014).

Main focus: first-principles strategies to study PL spectra of large solid-state systems

Outline

- Theory and First-principles Methodology
- Photoluminescence of All Inorganic Perovskites
- Photoluminescence of Point Defects in Semiconductors
- Summary and Outlook

Physical Processes and Approximations

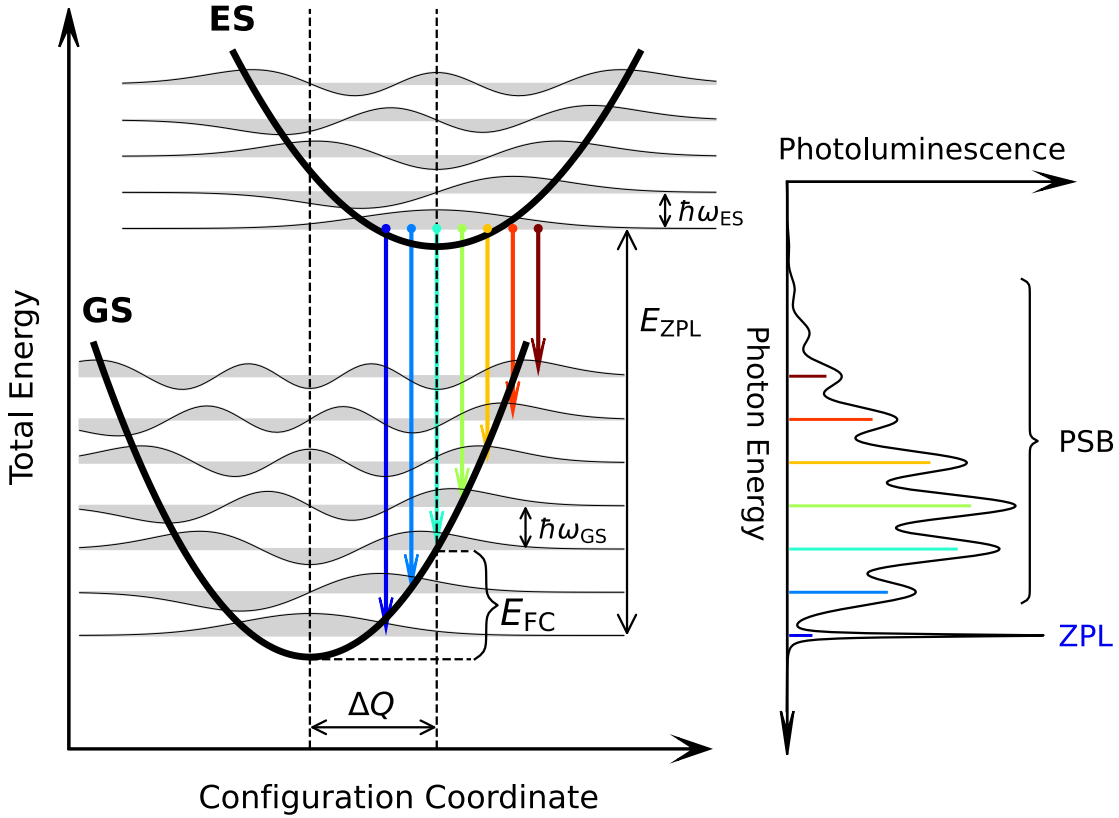

- **Fermi's golden rule**

$$I(\hbar\omega, T) \propto \sum_{m,n} P_m(T) \left| \langle \Phi_m | \hat{V} | \Phi_n \rangle \right|^2 \delta(\hbar\omega + E_m - E_n)$$

- Electric-dipole approximation, Born-Oppenheimer approximation, Franck-Condon (FC) approximation

Nuclear wavefunction

$$I(\hbar\omega, T) \propto \left| \boldsymbol{\mu}_{\mathrm{ES,GS}} \right|^2 \sum_{m,n} P_m(T) \left| \langle X_{\mathrm{ES},m} | \mathrm{X}_{\mathrm{GS,n}} \rangle \right|^2 \times$$
$$\delta\left(\hbar\omega + E_{\mathrm{GS},n} - E_{\mathrm{ES},m} - E_{\mathrm{ZPL}}\right)$$

Zero-phonon line (ZPL)

- **Franck-Condon (FC) shift**: $E_{\mathrm{FC}} \approx \frac{1}{2}\omega^2 \Delta Q^2$
- **Huang-Rhys factor (HRF):** $S = \frac{E_{\mathrm{FC}}}{\hbar\omega} = \frac{\omega \Delta Q^2}{2\hbar}$

PL with Weak Electron-Phonon (El-Ph) Coupling

Weak electron-phonon coupling: $S \approx 0$

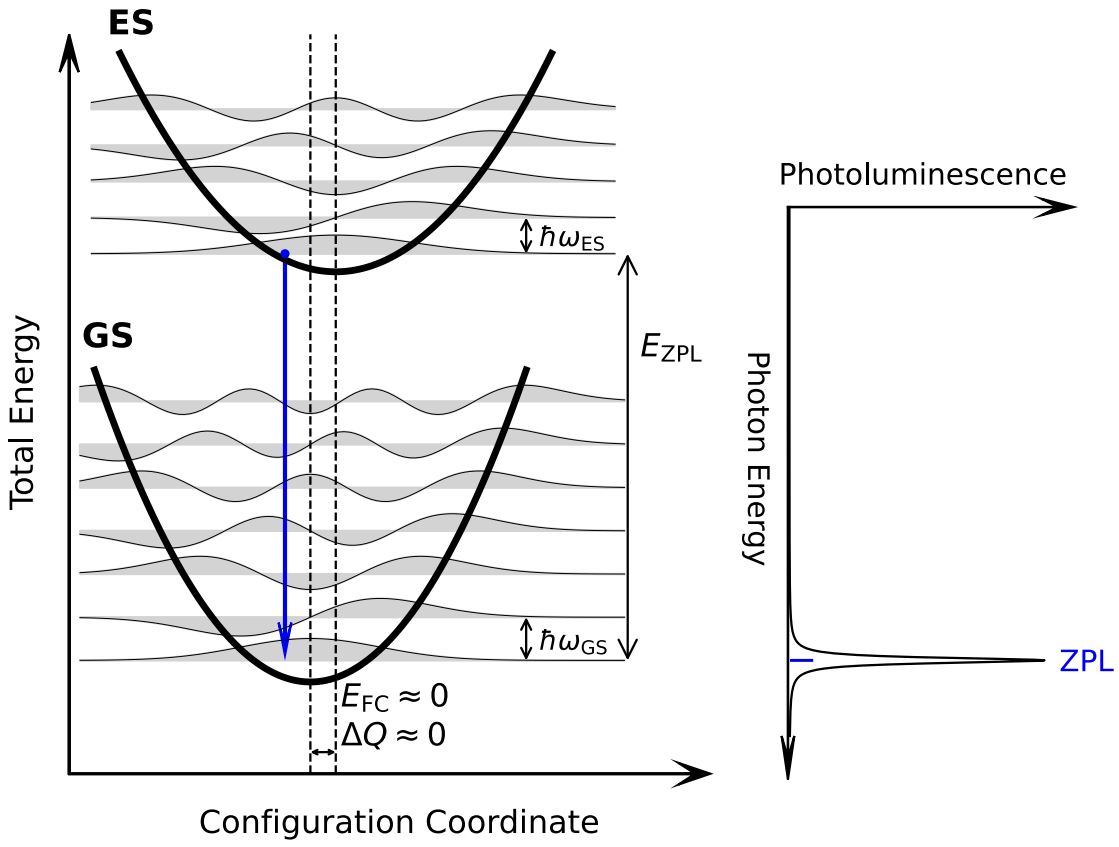

Example systems: pristine solids with delocalized excitons

$$I(\hbar\omega, T) \propto \left|\boldsymbol{\mu}_{\mathrm{ES,GS}}\right|^2 \delta(\hbar\omega - E_{\mathrm{ZPL}})$$

- Narrow PL line shape
- Same peak position for absorption and PL

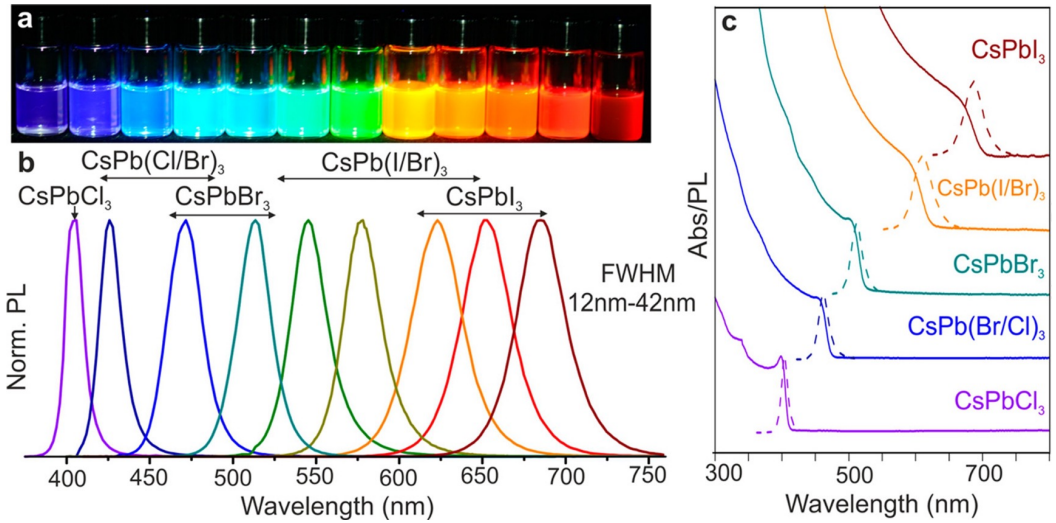

L. Protesescu et al., *Nano Lett*. **15**, 3692 (2015).

PL with Strong El-Ph Coupling

Strong electron-phonon coupling: $S \gg 1$

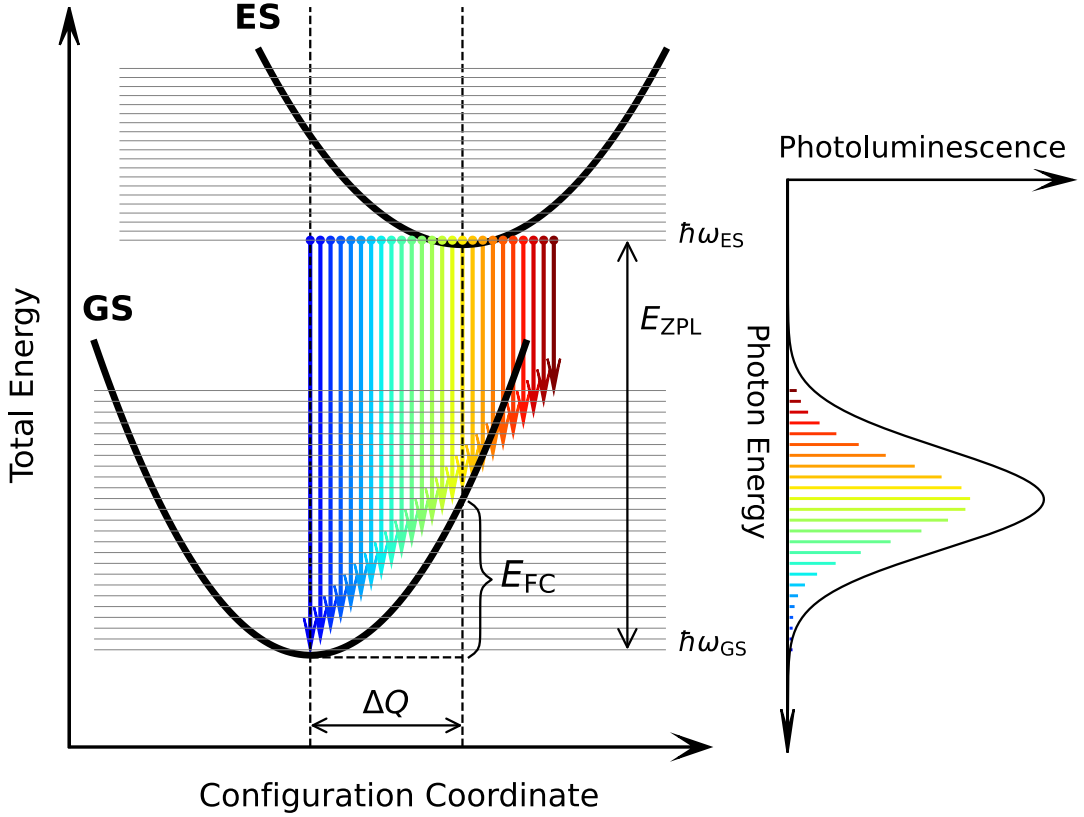

$$I(\hbar\omega, T) \propto \left|\boldsymbol{\mu}_{\mathrm{ES,GS}}\right|^2 \sum_{m,n} P_m(T) \left|\left\langle X_{\mathrm{ES},m} \middle| \mathrm{X}_{\mathrm{GS,n}} \right\rangle\right|^2 \times \delta\left(\hbar\omega + E_{\mathrm{GS},n} - E_{\mathrm{ES},m} - E_{\mathrm{ZPL}}\right)$$

Example systems: defects and self-trapped excitons in "soft" solids

- Broad PL line shape
- Different peak positions for absorption and emission

$Cs_2AgInCl_6$

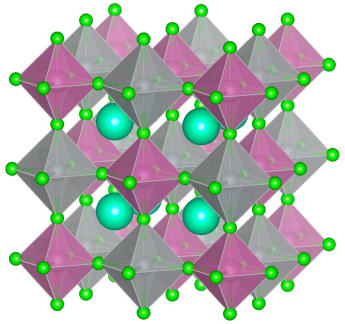

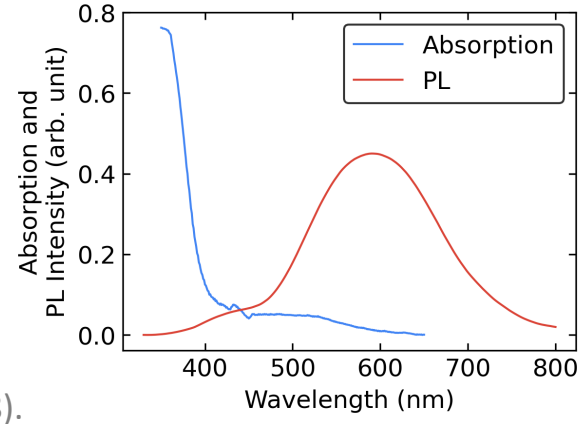

J. Luo et al., *Nature* **563**, 541 (2018).

PL with Strong El-Ph Coupling

1D configuration coordinate diagram (CCD)

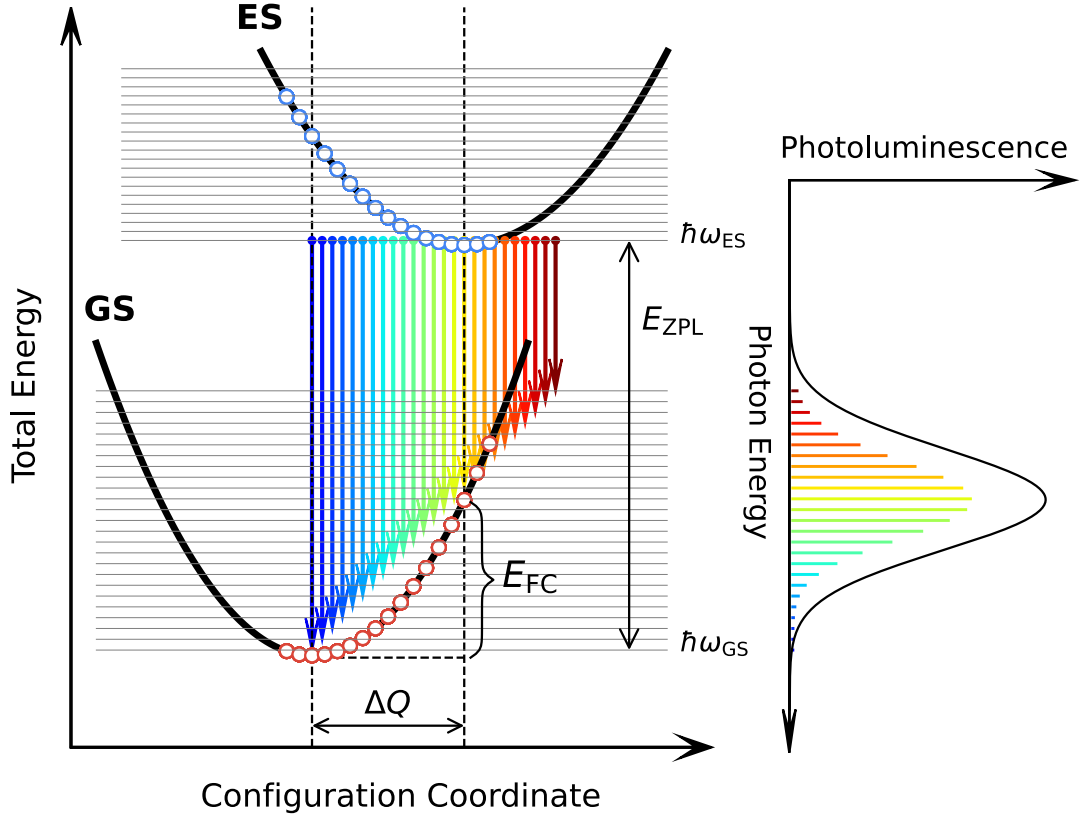

1. Optimize ground state (GS) and excited state (ES) geometries

2. Build the **1D CCD** as a **linear interpolation** between the GS and the ES geometries and calculate the energy profiles

$$\Delta Q = \left[\sum_{\alpha i} M_\alpha \Delta \boldsymbol{R}_{\alpha i}^2\right]^{1/2}$$

3. Calculate the **effective phonon modes** and the **Huang-Rhys factor (HRF)**

$$\hbar\omega_{\mathrm{GS}}, \qquad \hbar\omega_{\mathrm{ES}}, \qquad S = \frac{\omega_{\mathrm{GS}}\Delta Q^2}{2\hbar}$$

4. Compute the **FC integrals** and the PL

$$I_{mn} = \langle X_{\mathrm{ES},m}(Q - \Delta Q) | X_{\mathrm{GS},n}(Q) \rangle$$

P. T. Ruhoff, *Chem. Phys.* **186**. 355 (1994).

PL with Intermediate El-Ph Coupling

Intermediate electron-phonon coupling: $S \approx 1$

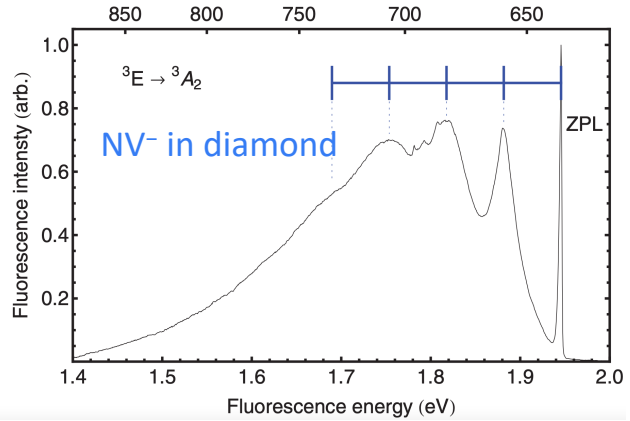

P. Kehayias et al., *Phys. Rev. B* **88**, 165202 (2013).

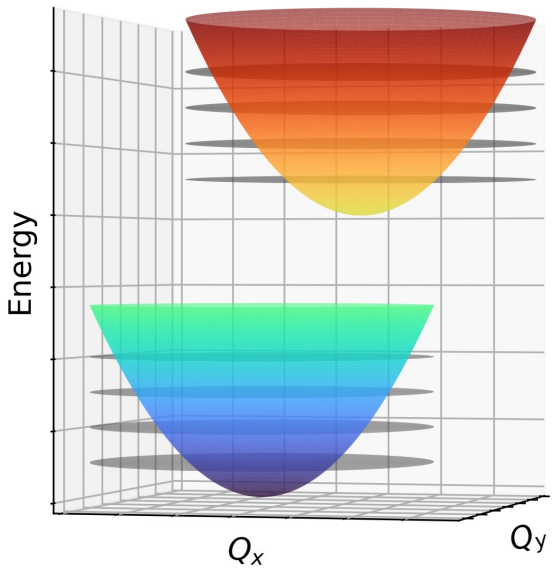

$$I(\hbar\omega, T) \propto \left|\boldsymbol{\mu}_{\mathrm{ES,GS}}\right|^2 \sum_{m,n} P_m(T) \left|\langle X_{\mathrm{ES},m} | \mathrm{X}_{\mathrm{GS,n}} \rangle\right|^2 \times \delta\left(\hbar\omega + E_{\mathrm{GS},n} - E_{\mathrm{ES},m} - E_{\mathrm{ZPL}}\right)$$

Example systems: point defects in "rigid" solids

- **Multidimensional** nuclear wavefunction in

$$|X_{\mathrm{ES},\{m\}}\rangle = \prod_k |\chi_{\mathrm{ES},km_k}\rangle, \quad |X_{\mathrm{GS},\{n\}}\rangle = \prod_k |\chi_{\mathrm{GS},kn_k}\rangle$$

- **Displaced harmonic oscillator approximation**

$$\hbar\omega_{\mathrm{ES},k} = \hbar\omega_{\mathrm{GS},k}$$

$$|\langle \chi_{k0}(Q_k - \Delta Q_k) | \chi_{kn}(Q) \rangle|^2 = \frac{S_k^n}{n!} \exp(-S_k)$$

- Partial Huang-Rhys factor (HRF): $S_k = \frac{\omega_k \Delta Q_k^2}{2\hbar}$

PL with Intermediate El-Ph Coupling

Generating function approach for PL line shape

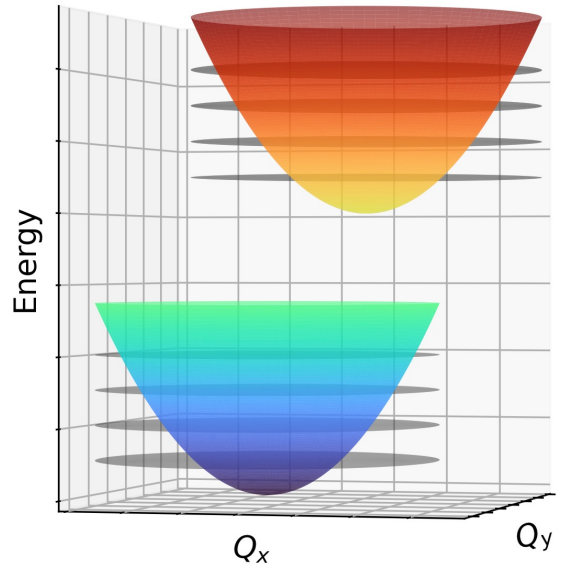

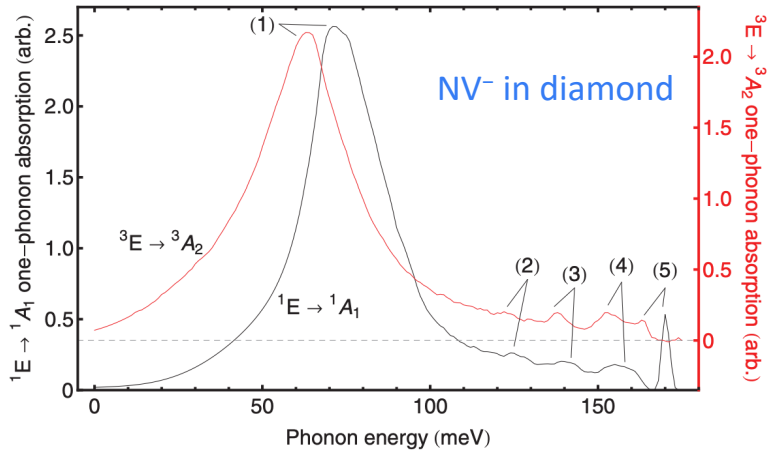

P. Kehayias et al., *Phys. Rev. B* **88**, 165202 (2013).

Energy of the zero-phonon line (ZPL)

$$I(\hbar\omega) \propto \frac{1}{2\pi\hbar}\int_{-\infty}^{\infty} \exp\left(i\omega t - \frac{iE_{\mathrm{ZPL}}t + \lambda|t|}{\hbar}\right) G(t)\mathrm{d}t$$

Broadening of the ZPL

- Generating function

$$G(t) = \exp[S(t) - S(0)]$$

- Spectral density of electron-phonon (el-ph) coupling

$$S(\hbar\omega) = \sum_k S_k \delta(\hbar\omega - \hbar\omega_k)$$

PL in Different El-Ph Coupling Regimes

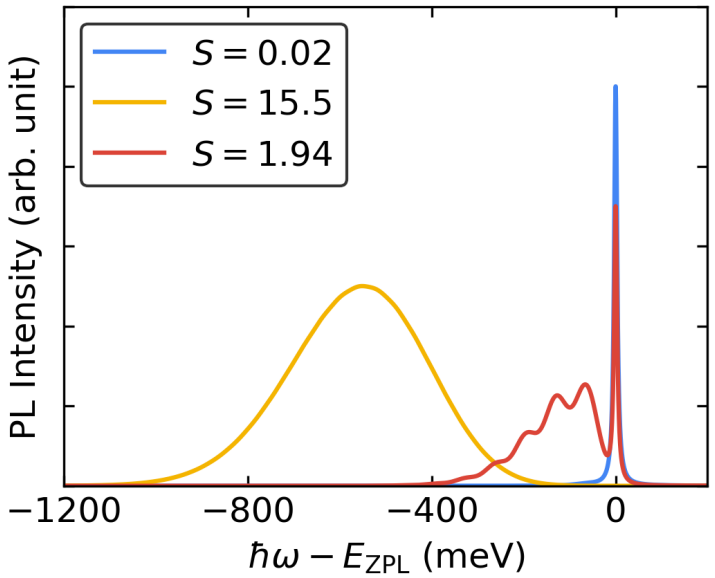

Coupling regimes	Weak coupling: $S \approx 0$	Strong coupling: $S \gg 1$	Intermediate coupling: $S \approx 1$
Features	Narrow PL $E_{\mathrm{abs}} \approx E_{\mathrm{emi}}$	Broad PL $E_{\mathrm{abs}} - E_{\mathrm{emi}} \approx 2S\hbar\omega_{\mathrm{eff}}$	Zero-phonon line & phonon side band
Computation	Gaussian or Lorentzian peak at E_{emi}	1D CCD, effective modes, FC integrals	All modes, generating function
Example systems	Pristine solids with delocalized exciton	Self-trapped exciton in perovskites	Point defects in semiconductors

Outline

- Theory and First-principles Methodology
- Photoluminescence of All Inorganic Perovskites
- Photoluminescence of Point Defects in Semiconductors
- Summary and Outlook

Self trapped exciton and broadband PL

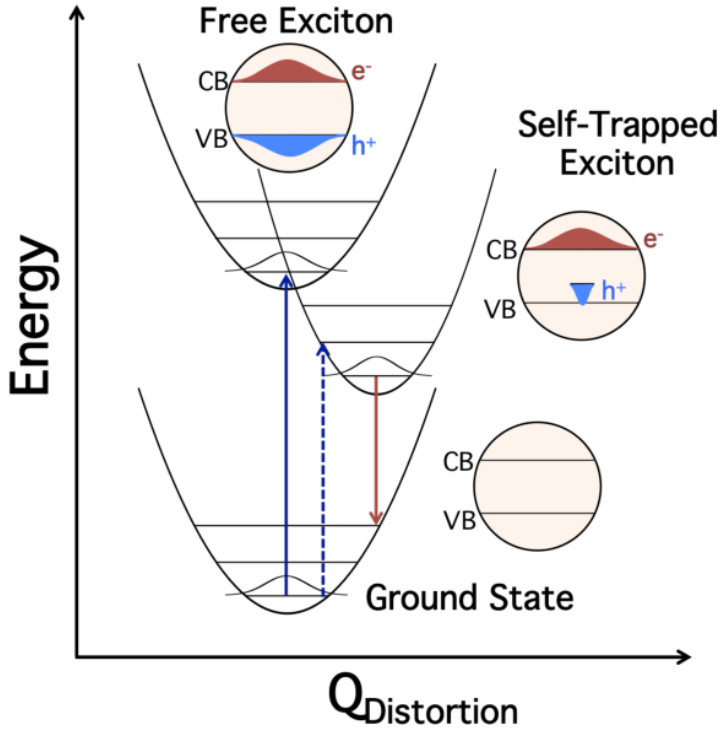

K. E. Knowles et al., *J. Am. Chem. Soc.* **137**, 13138 (2015).

After absorbing the light free exciton is relaxed (stabilized) into a **self trapped exciton (STE)**

Systems with STE exhibit **broadband PL** and large Franck-Condon shifts

Potential application: lead-free white light source

$Cs_2AgInCl_6$

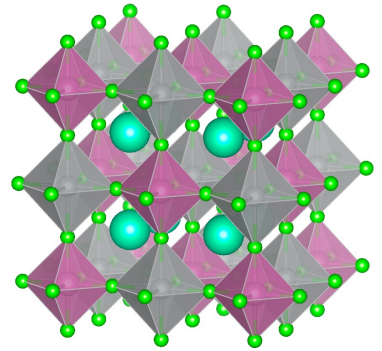

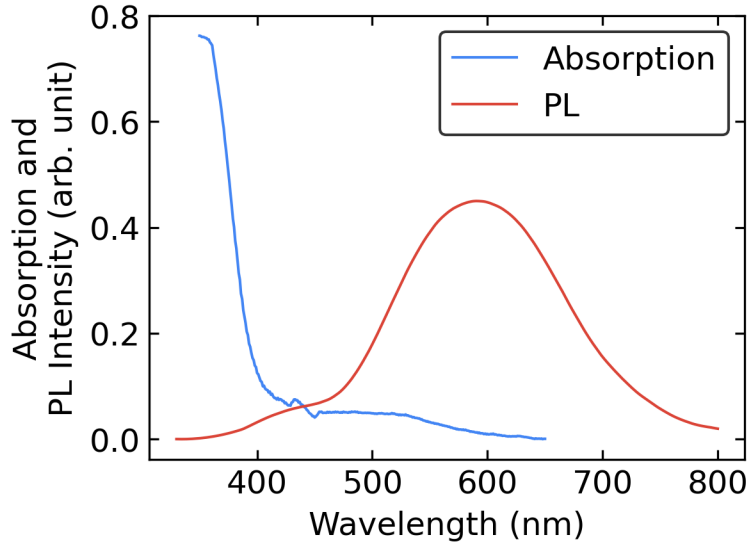

J. Luo et al., *Nature* **563**, 541 (2018).

First-principles Calculations

1. Build the structural model for the perovskite
   - supercell with periodic boundary condition

2. DFT study of the ground state (GS)
   - **GS atomic geometry**

3. CDFT (ΔSCF) or ROKS study of the excited state (ES)
   - **ES atomic geometry** and $\boldsymbol{E_{ZPL}}$

4. Build the **1D configuration coordinate diagram (CCD)** between the GS and the ES geometries
   - **Atomic displacement**
   - **Effective phonon modes**

5. Compute the **FC integrals** and the PL

$(2 \times 2 \times 2)$ supercell of $Cs_2AgInCl_6$ with 320 atoms

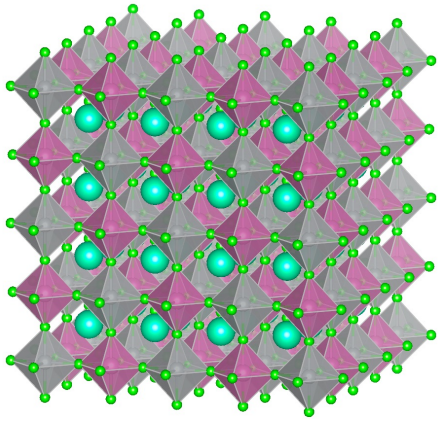

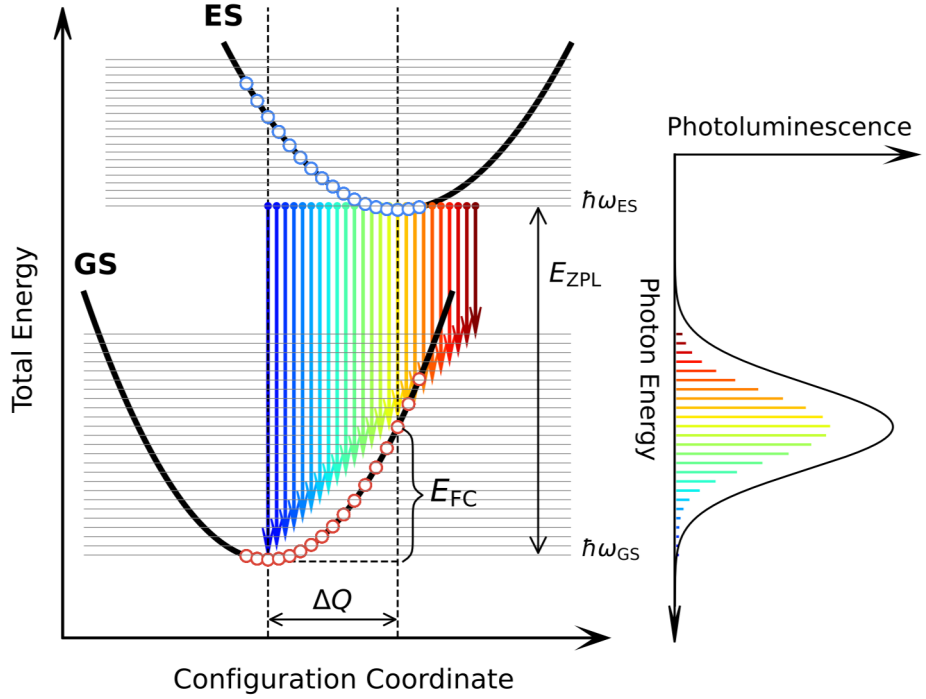

J. Luo et al., *Nature* **563**, 541 (2018).
X. Wang et al., *J. Phys. Chem. Lett*. **10**, 501 (2019).

1D CCD and the Broadband PL

The broad PL from the **self-trapped exciton** originates from the **strong electron-phonon coupling**

ΔQ (amu$^{0.5}$ Å)	$\hbar\omega_{GS}$ (meV)	$\hbar\omega_{ES}$ (meV)	S_{GS}	S_{ES}
4.35	18.3	17.4	37	30

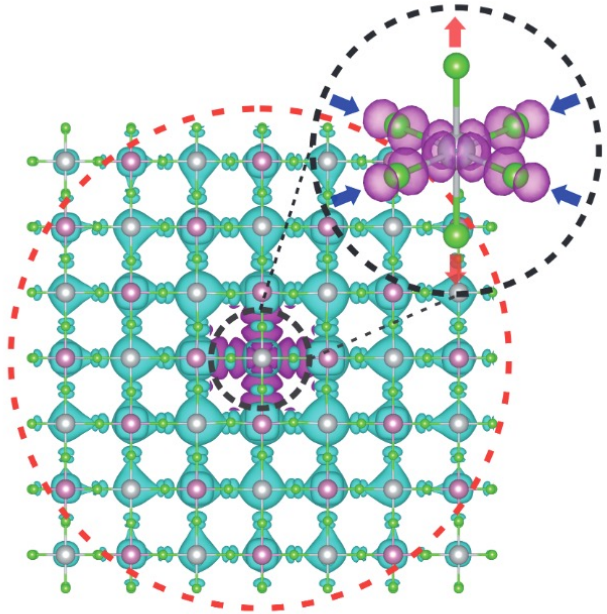

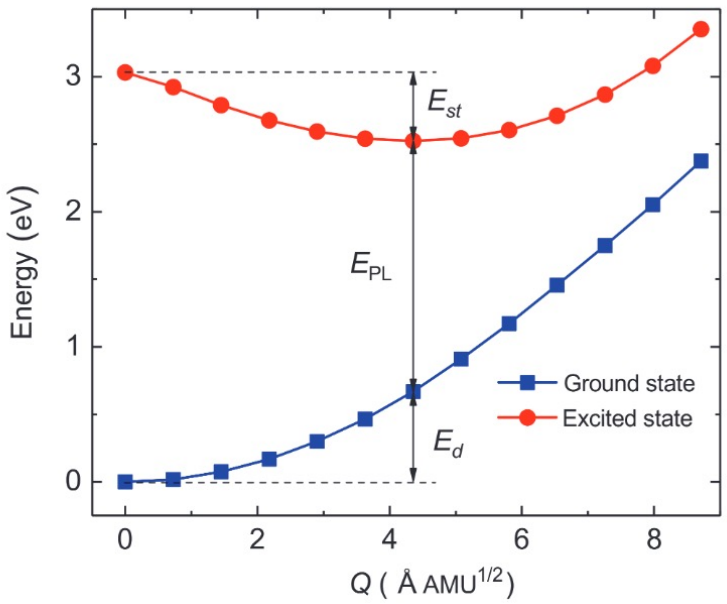

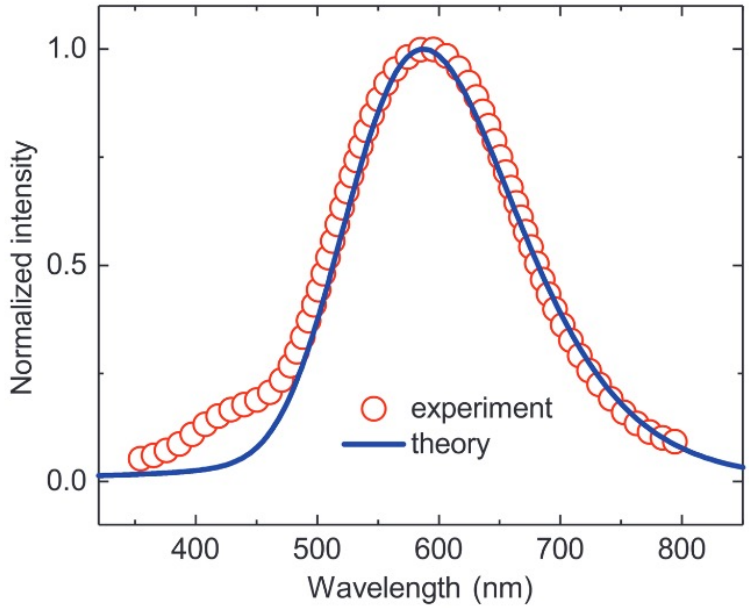

J. Luo et al., *Nature* **563**, 541 (2018).
X. Wang et al., *J. Phys. Chem. Lett*. **10**, 501 (2019).

Outline

- Theory and First-principles Methodology
- Photoluminescence of All Inorganic Perovskites
- Photoluminescence of Point Defects in Semiconductors
- Summary and Outlook

PL of Point Defects in Semiconductors

Optically active point defects in semiconductors are potential platforms for quantum technology applications

Nitrogen-vacancy (NV^-) center in diamond

A. Gali, *Nanophotonics* **8**, 1907 (2019).
C. E. Dreyer et al., *Annu. Rev. Mater. Res*. **48**, 1 (2018).

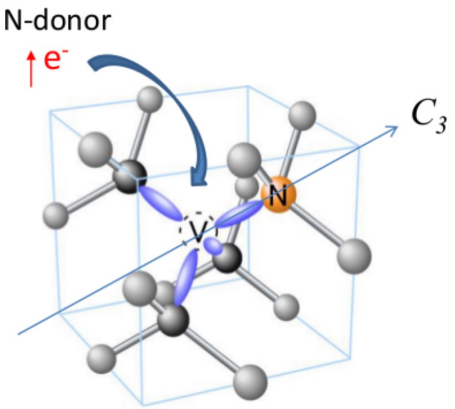

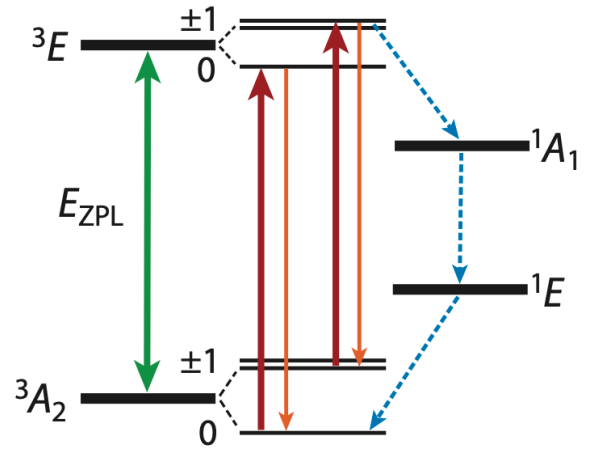

- **Characterization**
- **Design of spin qubits**

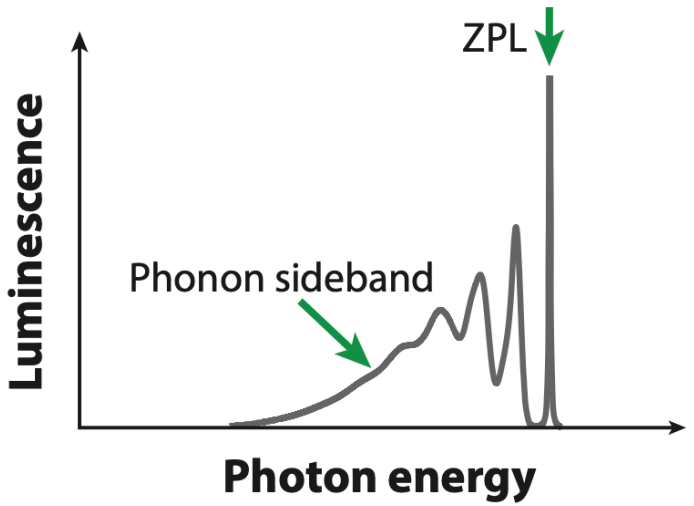

First-principles Calculations

1. Build the structural model for the defect
   - supercell with periodic boundary condition
2. DFT study of the ground state (GS)
   - **GS atomic geometry**
   - **All phonon modes**
3. CDFT (ΔSCF) or TDDFT study of the excited state (ES)
   - **ES atomic geometry**
   - Energy of the **zero-phonon line: E_{ZPL}**
4. Compute PL using the **generating function approach**

NV^- center in a (4 × 4 × 4) supercell of diamond with 512 atomic sites

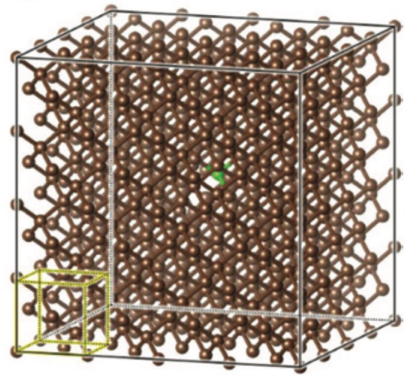

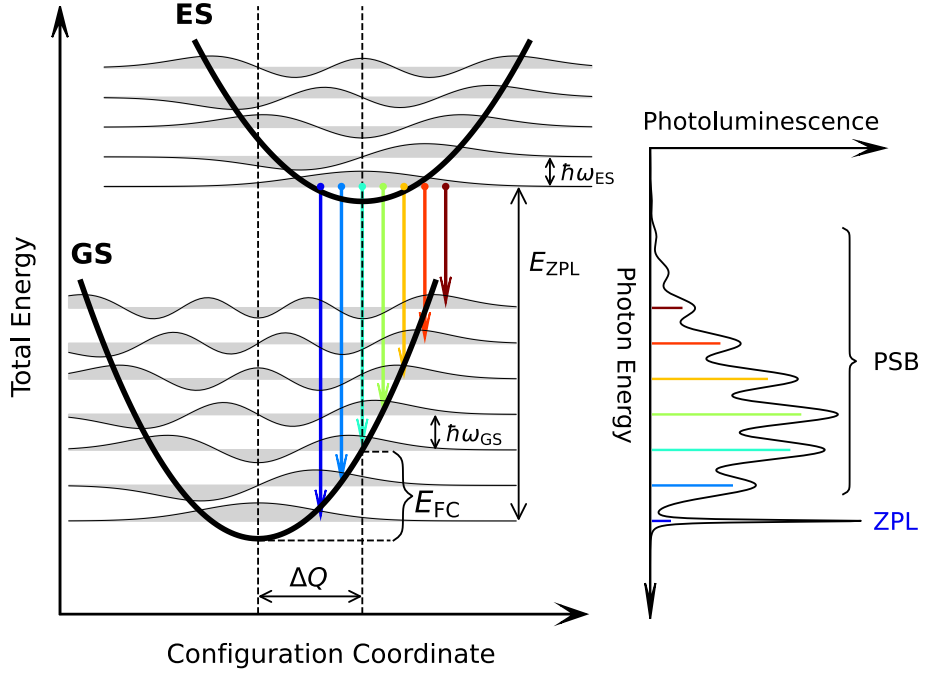

Y. Jin, M. Govoni et al., *Phys. Rev. Mater.* 5, 084603 (2021).

PL Line Shape of NV^- in Diamond

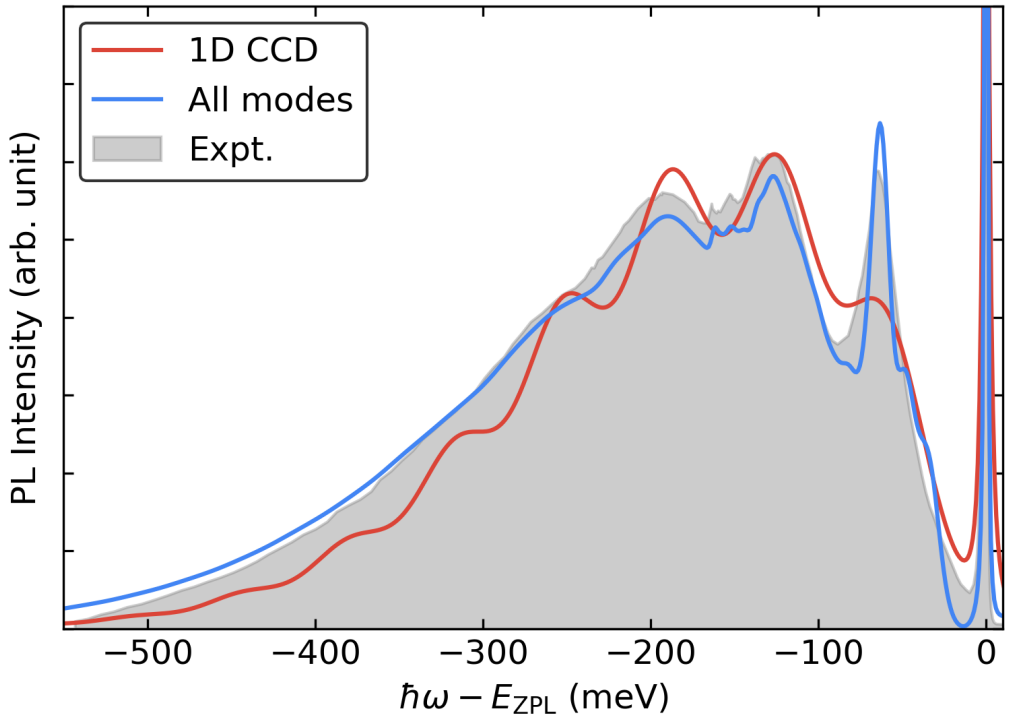

- 1D CCD can't capture the details of the PL line shape
- The PL line shape predicted using all vibrational modes are in better agreement with the experiment
- **Finite size effects**
  - Underestimate of intensity at around -20 meV
  - Shoulder peaks around -50 meV

Extrapolating to the Dilute Limit

$$\Delta Q_k = \frac{1}{\omega_k^2} \sum_{\alpha=1}^{N} \sum_{i=x,y,z} \frac{\boldsymbol{F}_{\alpha i}}{\sqrt{M_\alpha}} \boldsymbol{e}_{k,\alpha i}$$

Atomic forces ($\boldsymbol{F}_{\alpha i}$) outside the sphere are negligible

($4 \times 4 \times 4$) supercell

($N \times N \times N$) supercell

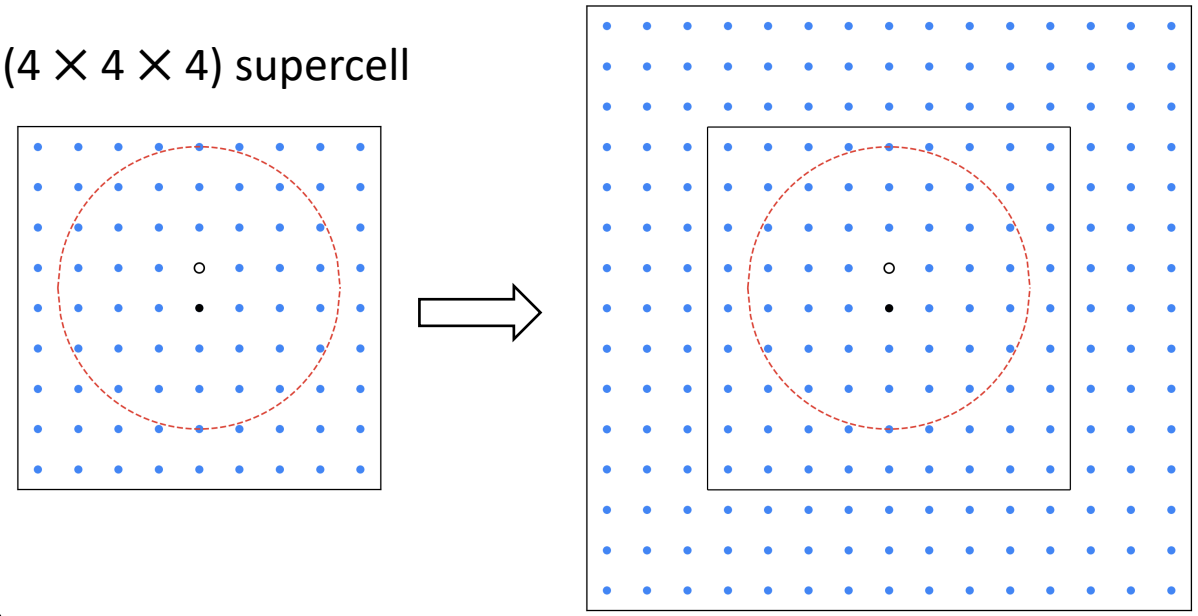

Force constant matrix ($\boldsymbol{D}$) embedding approach

- If both atoms are within the sphere, then the matrix element of the small defect supercell is used
- If two atoms are separated by a distance larger than a chosen cutoff radius, then the matrix element is set to zero
- For all other atom pairs, the values of the pristine bulk system is used

$\boldsymbol{D}$ (defect in small supercell) $\boldsymbol{D}$ (pristine bulk supercell)

$\boldsymbol{D}$ (defect in large supercell)

$$\boldsymbol{D}\boldsymbol{e}_k = \omega_k^2 \boldsymbol{e}$$

A. Alkauskas et al., *New J. Phys*. **24**, 073026 (2014). L. Razinkovas et al., *Phys. Rev. B* **104**, 045303 (2021).

Spectral Density of El-Ph Coupling

Total Huang-Rhys factor (HRF)

$$S = \sum_k S_k = \sum_k \frac{\omega_k \Delta Q_k^2}{2\hbar}$$

Spectral density of electron-phonon coupling

$$S(\hbar\omega) = \sum_k S_k \delta(\hbar\omega - \hbar\omega_k)$$

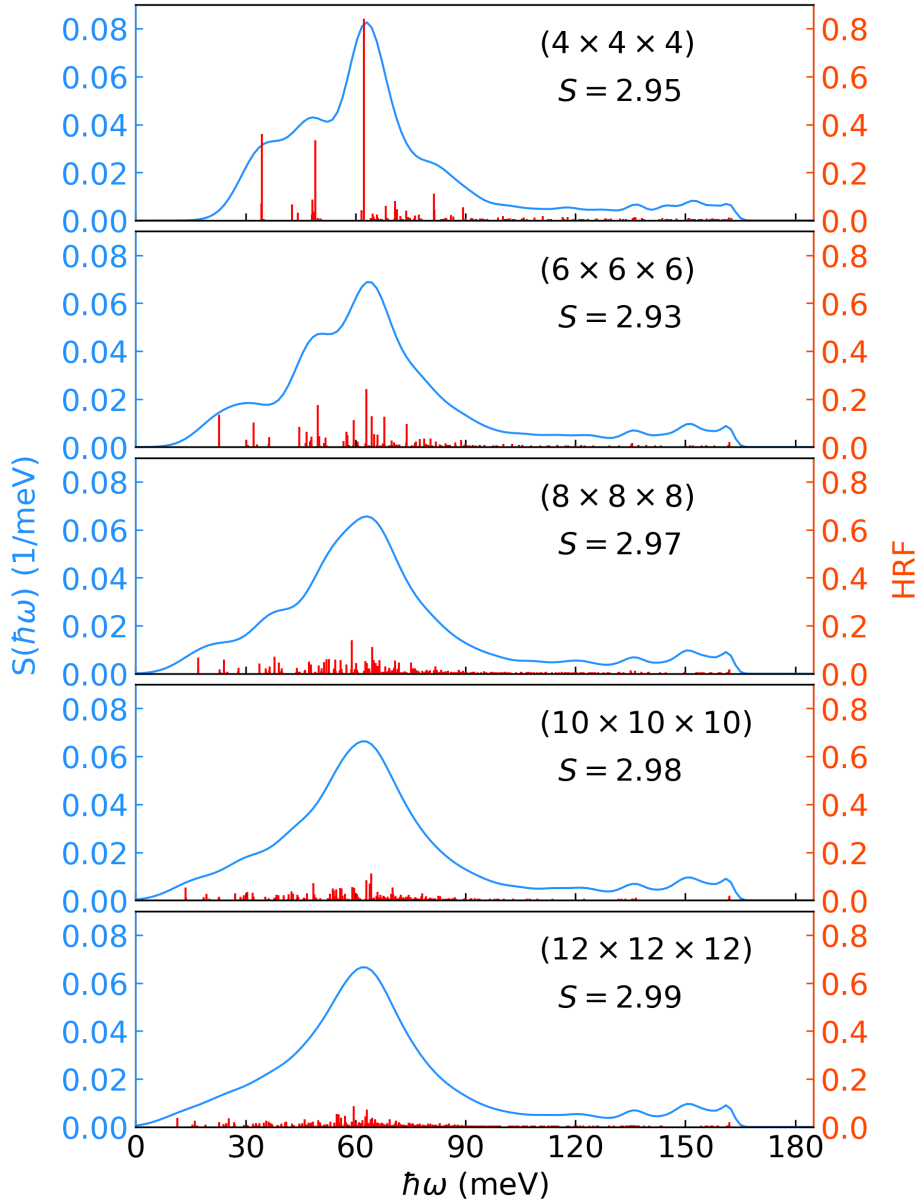

For NV^- center in diamond, extrapolating to the dilute limit

- smooths the spectral density
- includes the contribution of **long-range phonons**

Vibrational Modes Analysis

Inverse partition function (IPR)

$$\mathrm{IPR}_k = \frac{1}{\sum_{\alpha=1}^{N}\left(\sum_{i=x,y,z} \boldsymbol{e}_{k,\alpha i}^2\right)^2}$$

Localization factor (β)

$$\beta_k = \frac{N}{\mathrm{IPR}_k}$$

- **Quasi-local vibrational modes** at 65 meV
- **Localized vibrational modes** at 162 meV

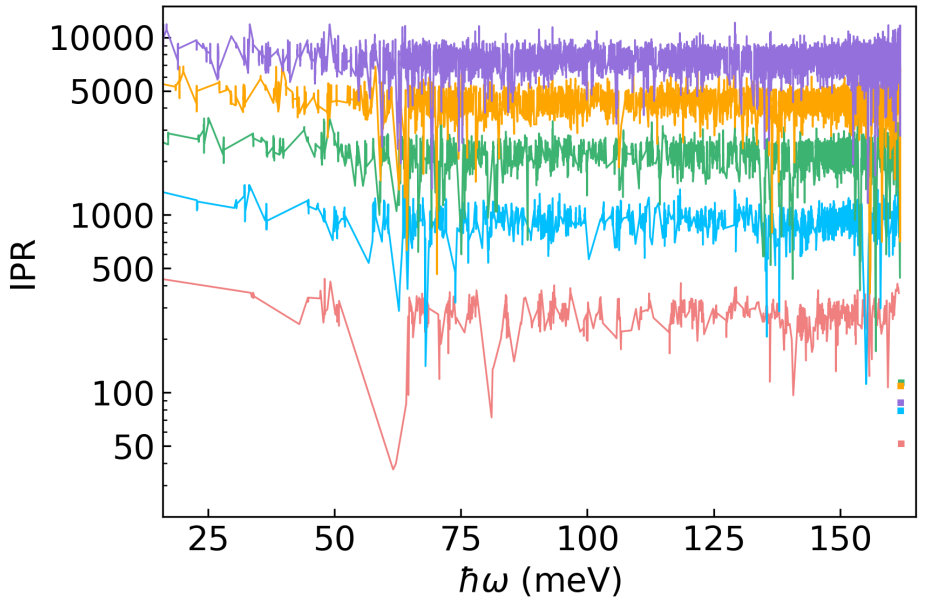

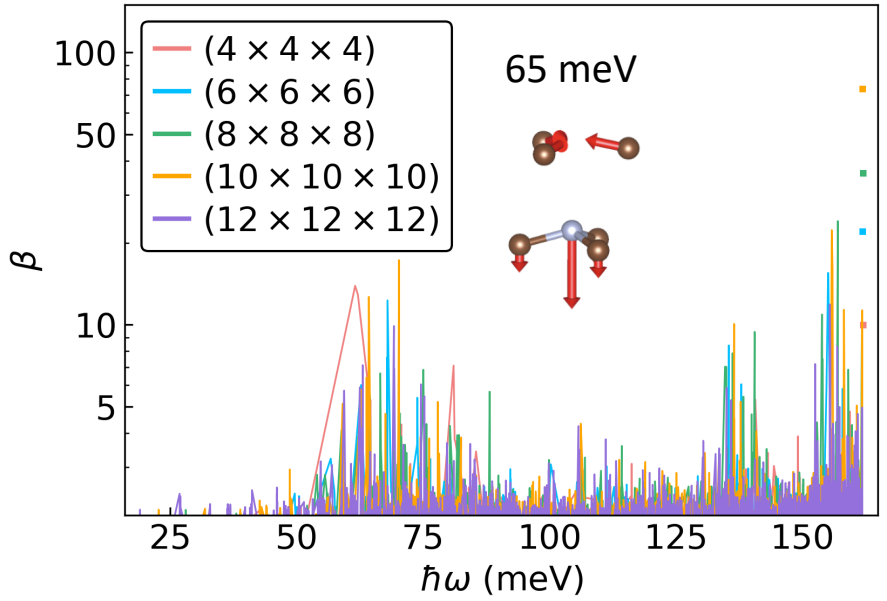

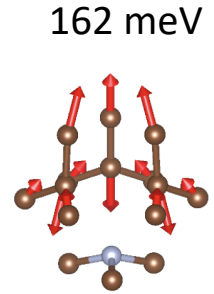

PL Line Shape at the Dilute Limit

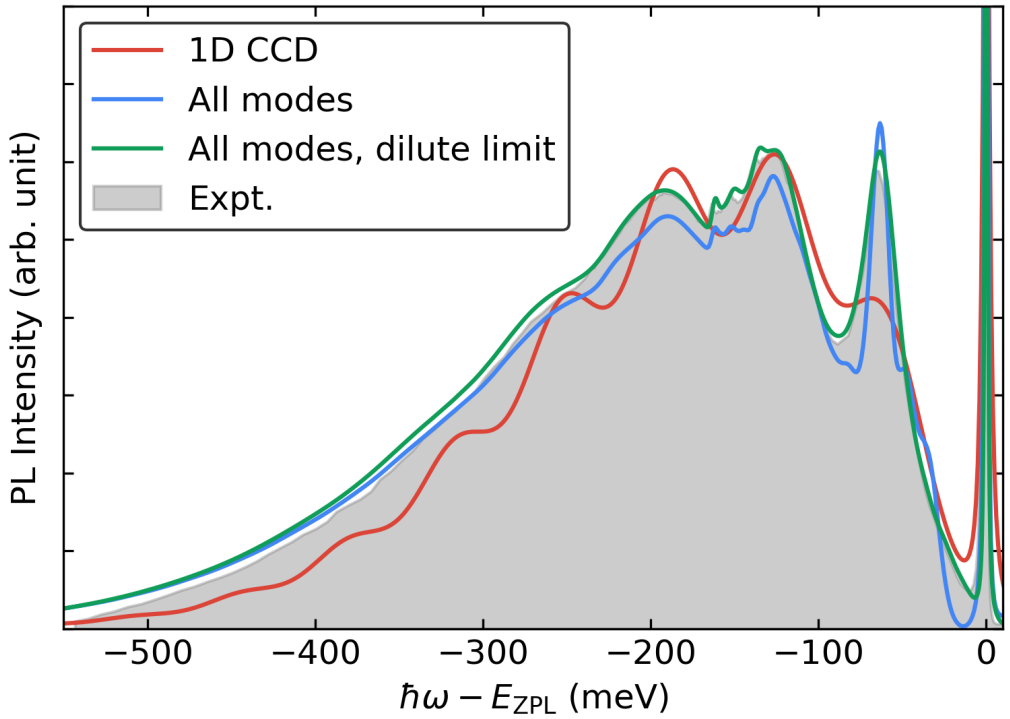

The agreement between the theoretical and experimental PL line shapes is significantly improved by extrapolating to the dilute limit

- Phonon side band dominates by the coupling with the 65 meV quasi-local vibrational mode
- Detailed features at ~125, 140, 155 and 165 meV are correctly predicted
- Contributions of long-range phonons are included

Comparison of Different Functionals

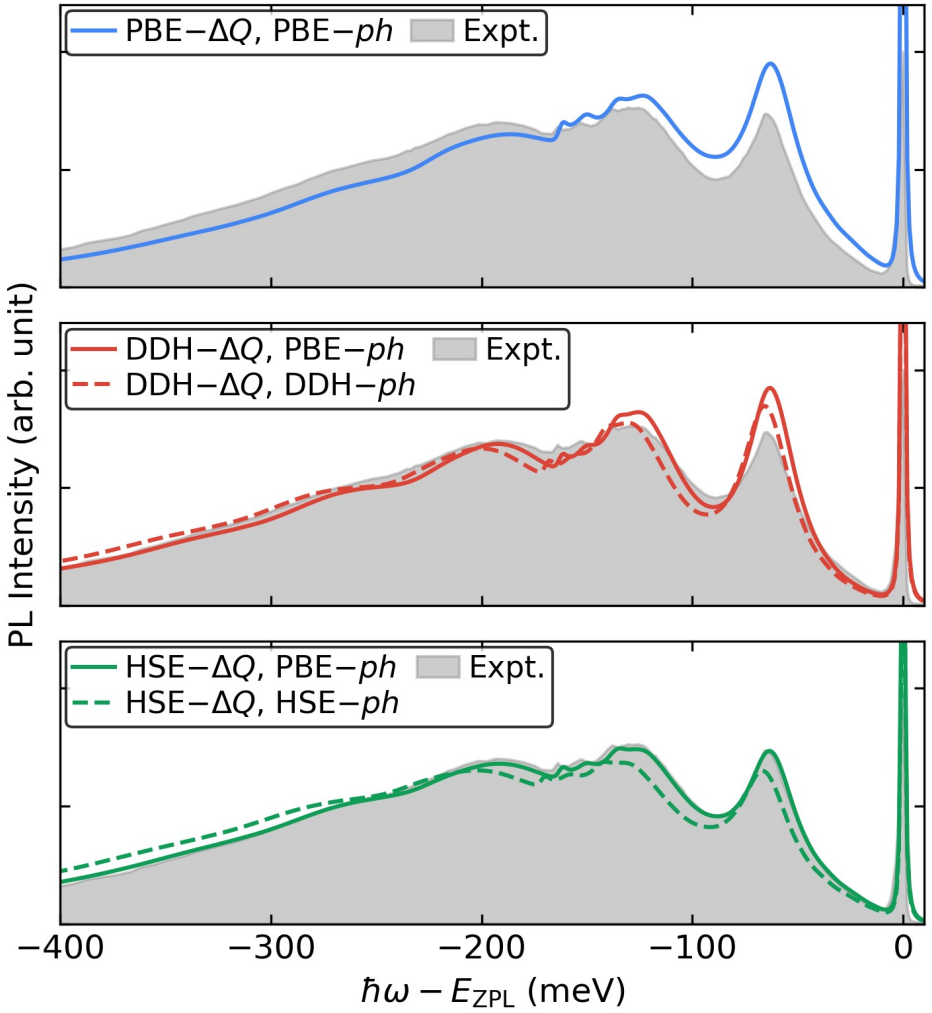

Debye-Waller factor: $\mathrm{DWF} \approx \exp(-S)$

	PBE-ΔQ	DDH-ΔQ		HSE-ΔQ		Expt.
	PBE-*ph*	PBE-*ph*	DDH-*ph*	PBE-*ph*	HSE-*ph*	
DWF (%)	5.0	4.1	3.7	**3.0**	2.5	3.2

- Energies of PBE phonons are in the best agreement with the experiment
- HSE predicts the relative intensity the best
- **HSE-ΔQ with PBE-*ph* yields the line shape and the DWF in the best comparison with the experiment**

P. Kehayias, D. Budker et al., *Phys. Rev. B* 88, 165202 (2013).
Y. Jin, M. Govoni et al., *Phys. Rev. Mater.* 5, 084603 (2021).

Temperature Dependent PL

Temperature effect can be included through the **average occupations** of vibrational levels in the excited state

$$F(t,T) = \exp[S(t) - S(0) + C(t,T) + C(-t,T) - 2C(0,T)]$$

$$C(\hbar\omega, T) = \sum_k \overline{n}_k(T) S_k \delta(\hbar\omega - \hbar\omega_k)$$

ZPL broadening as a function of temperature

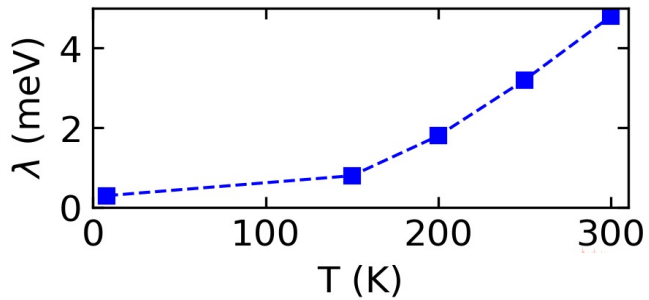

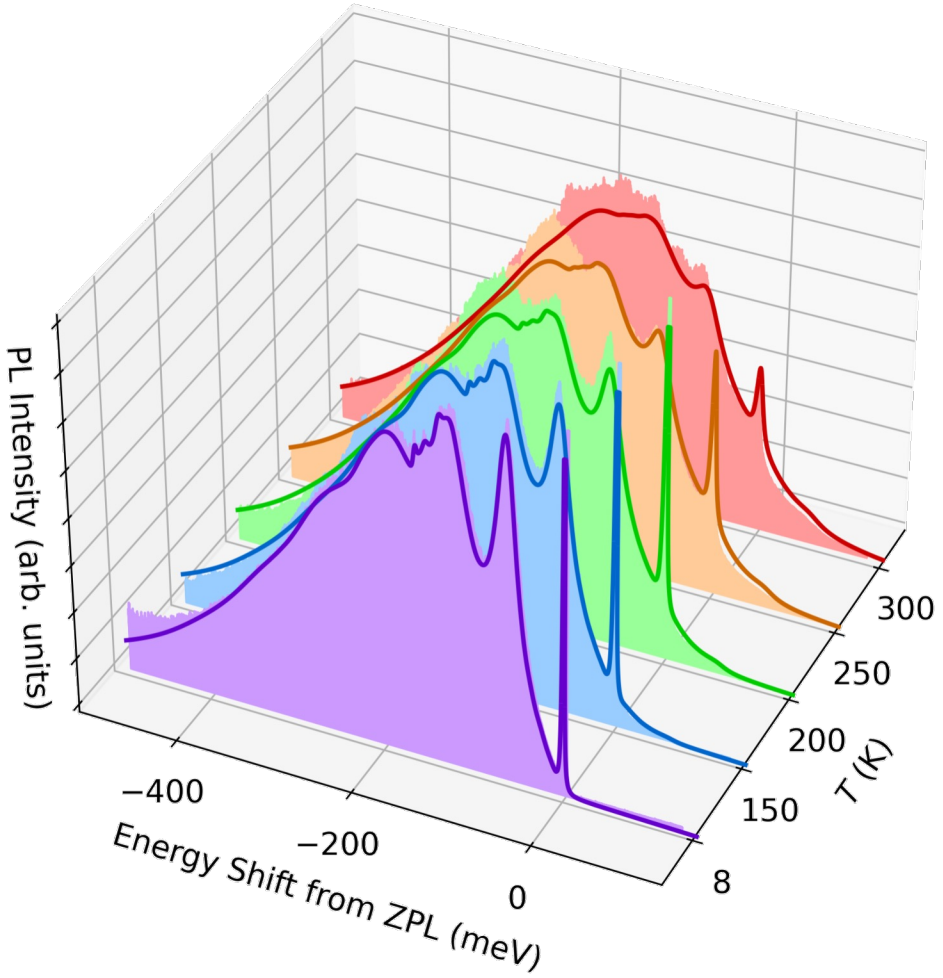

Y. Jin, M. Govoni et al., *Phys. Rev. Mater.* 5, 084603 (2021).

Absorption between Singlet States

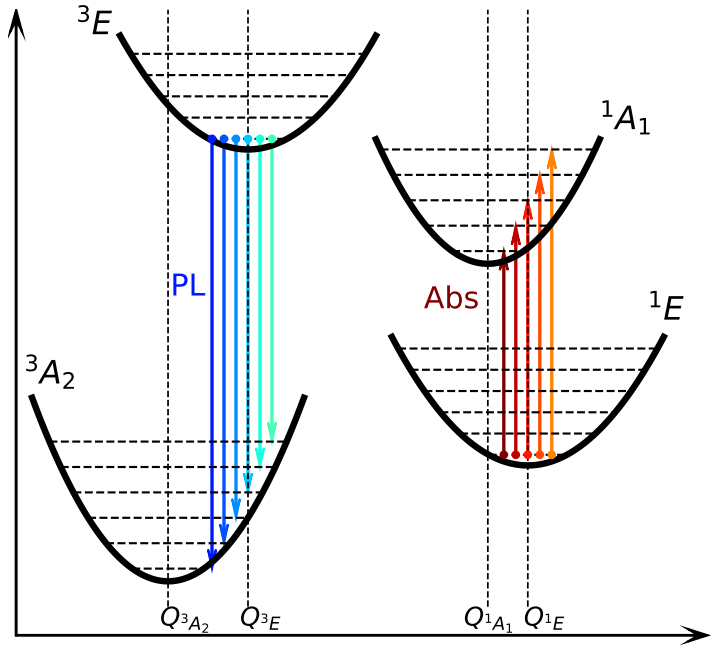

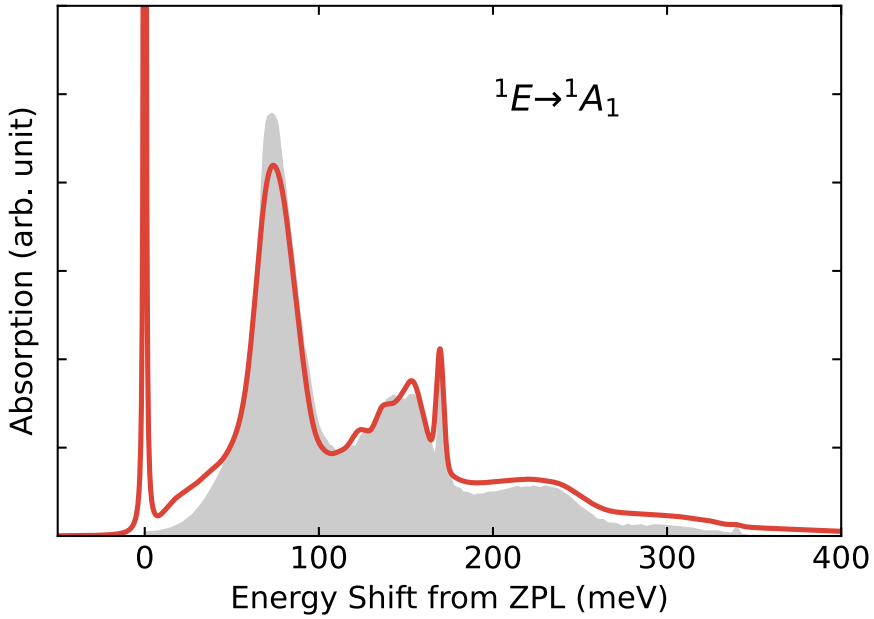

P. Kehayias et al., *Phys. Rev. B* **88**, 165202 (2013).

- Geometries and vibrational modes of the strongly-correlated $^1A_1$ and ^1E states are studied using **spin-flip TDDFT with analytical nuclear gradients** implemented in the WEST code

Y. Jin, M. Govoni, and G. Galli, arXiv:2208.04504 (2022).

Outline

- Theory and First-principles Methodology
- Photoluminescence of All Inorganic Perovskites
- Photoluminescence of Point Defects in Semiconductors
- Summary and Outlook

Summary

PL spectra of solid-state systems can be characterized using first-principles approaches

Light emitting all inorganic perovskites

- Formation of self trapped exciton (STE)
- **1D configuration coordinate diagram (CCD)**

J. Luo et al., *Nature* **563**, 541 (2018).
X. Wang et al., *J. Phys. Chem. Lett*. **10**, 501 (2019).

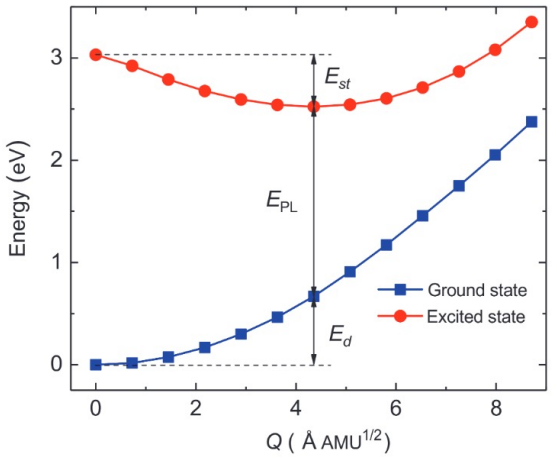

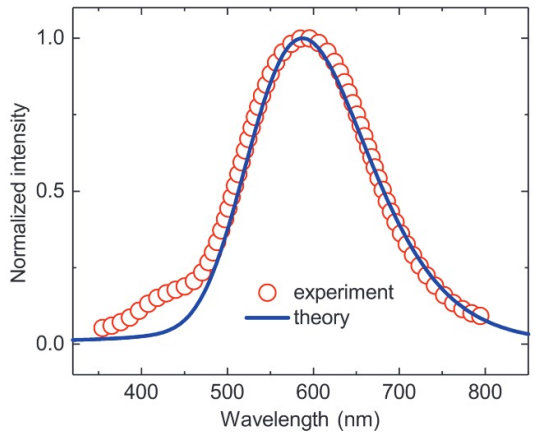

Point defects in semiconductors

- Coupling between the optical transition and all vibrational modes
- **Generating function approach** for the line shape at finite temperature
- **Force constant matrix embedding approach** for finite-size effects

Y. Jin, M. Govoni et al., *Phys. Rev. Mater.* 5, 084603 (2021).
Y. Jin, M. Govoni, and G. Galli, arXiv:2208.04504 (2022).

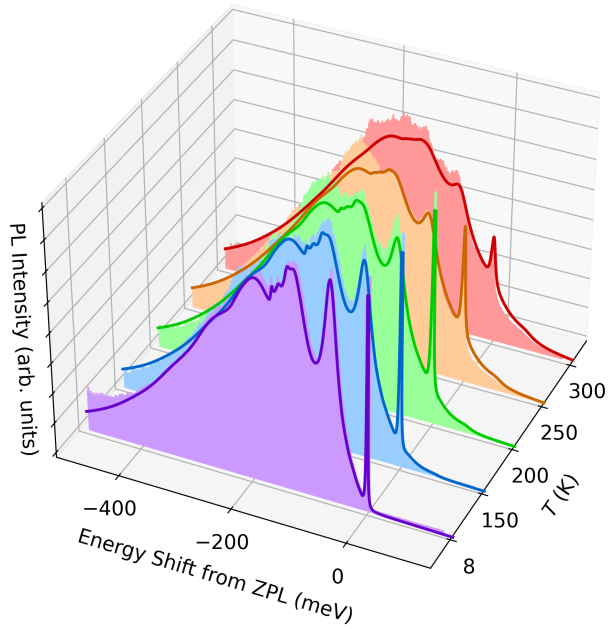

Outlook

Future work: method development for excited state potential energy surfaces

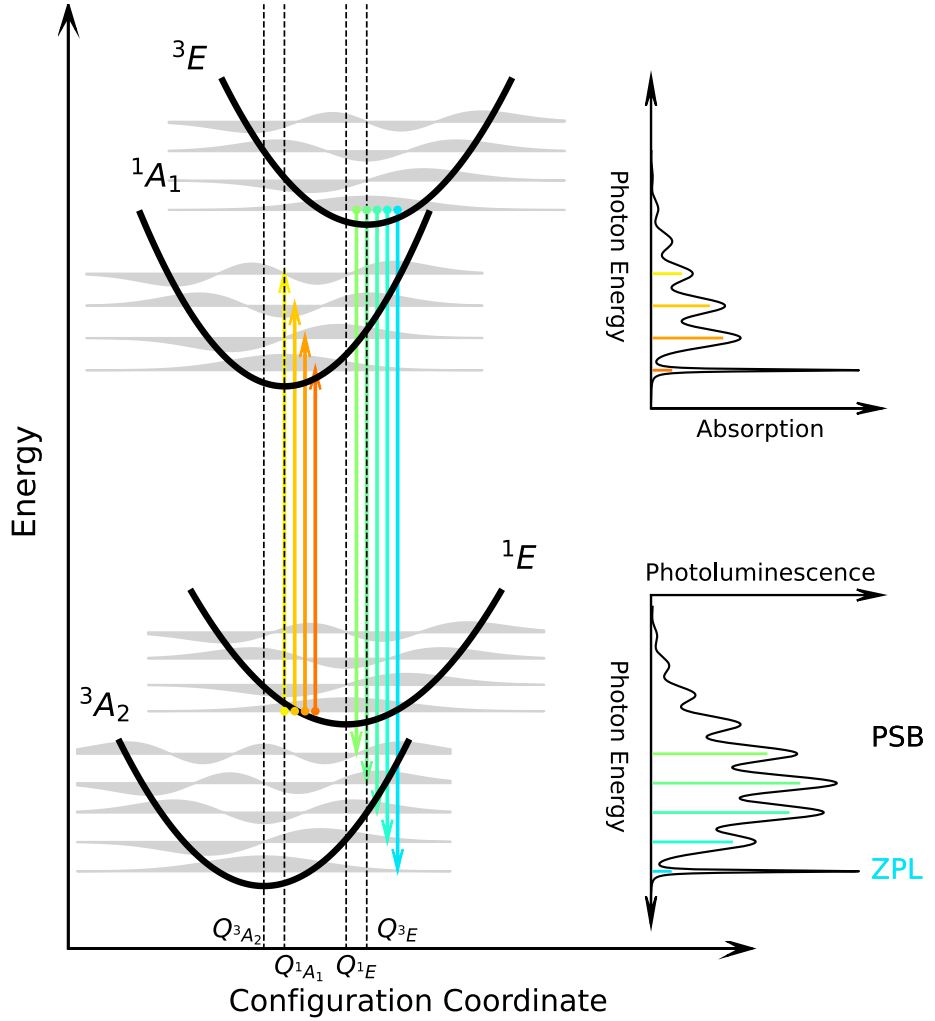

Methods based on DFT (CDFT, TDDFT)

- More rigorous treatment of excited states
- More accurate density functionals

Methods based on many-body perturbation theory (*GW*-BSE, QDET)

- Implementation of analytical nuclear forces

Quantum chemistry methods

- Implementation with periodic boundary condition
- Reducing the computational cost to enable calculations for large systems

Outlook

Future work: beyond the approximations in the calculation of PL spectra

Non-Born-Oppenheimer effect and the anharmonicity

BO: $|\Phi_m\rangle = |\Psi\rangle|X_m\rangle$

Non-BO: $|\Phi_m\rangle = \sum_i (c_{mi}|\Psi_1\rangle|X_i\rangle + d_{mi}|\Psi_2\rangle|X_i\rangle)$

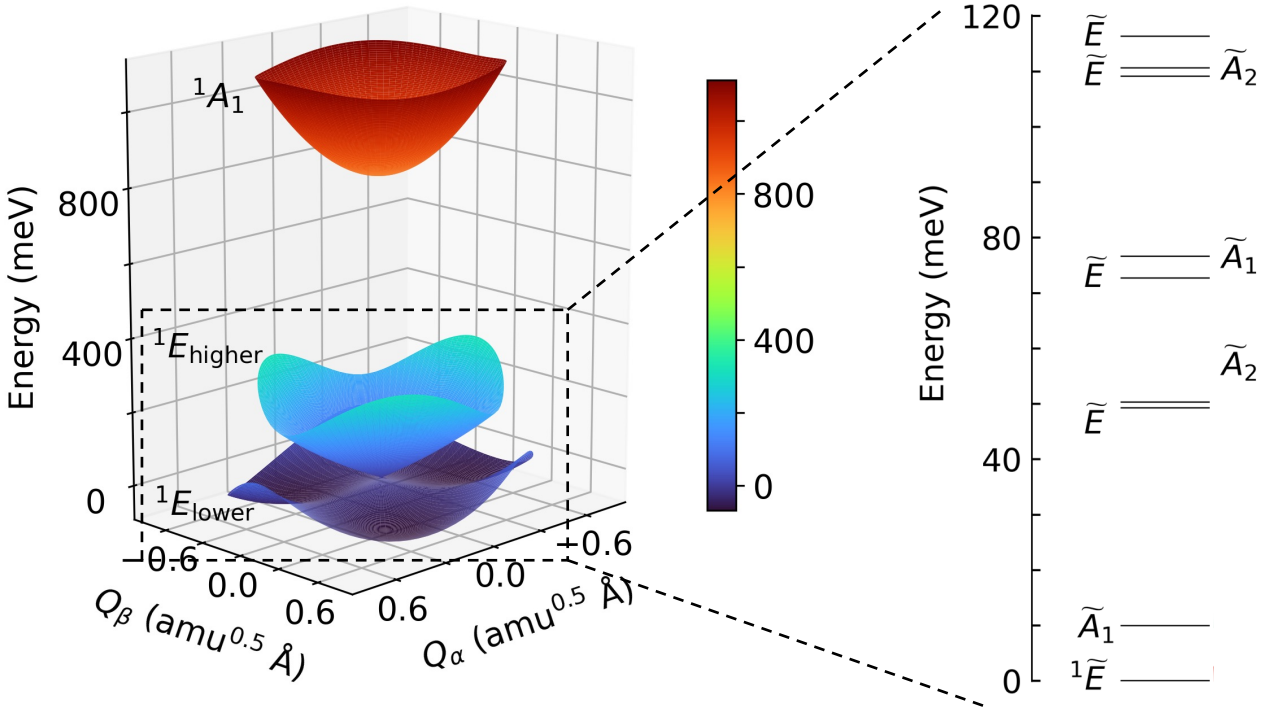

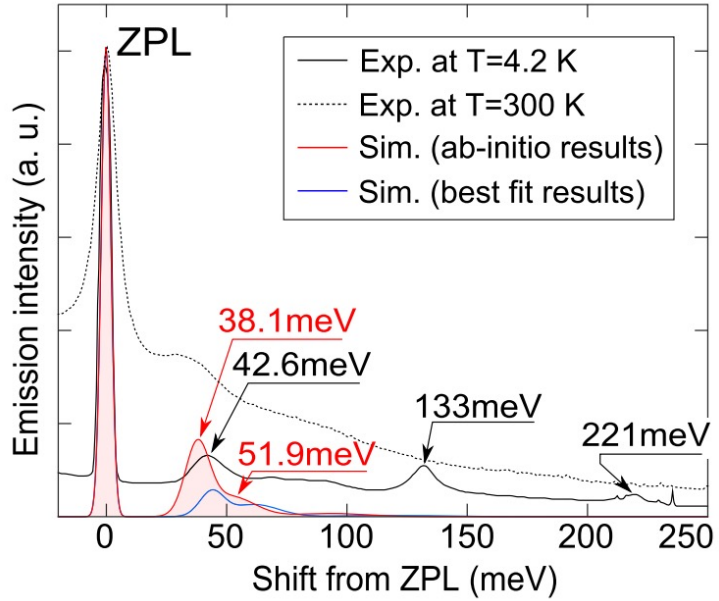

Y. Jin, M. Govoni, and G. Galli, arXiv:2208.04504.
G. Thiering and A. Gali, *Phys. Rev. B* **98**, 085207 (2018).
L. Razinkovas et al., *Phys. Rev. B* **104**, 045303 (2021).

Outlook

Future work: beyond the approximations in the calculation of PL spectra

Herzberg-Teller effect

$$\boldsymbol{\mu} = \boldsymbol{\mu}_0 + \sum_k \left(\frac{\partial \boldsymbol{\mu}}{\partial Q_k}\right) \Delta Q_k$$

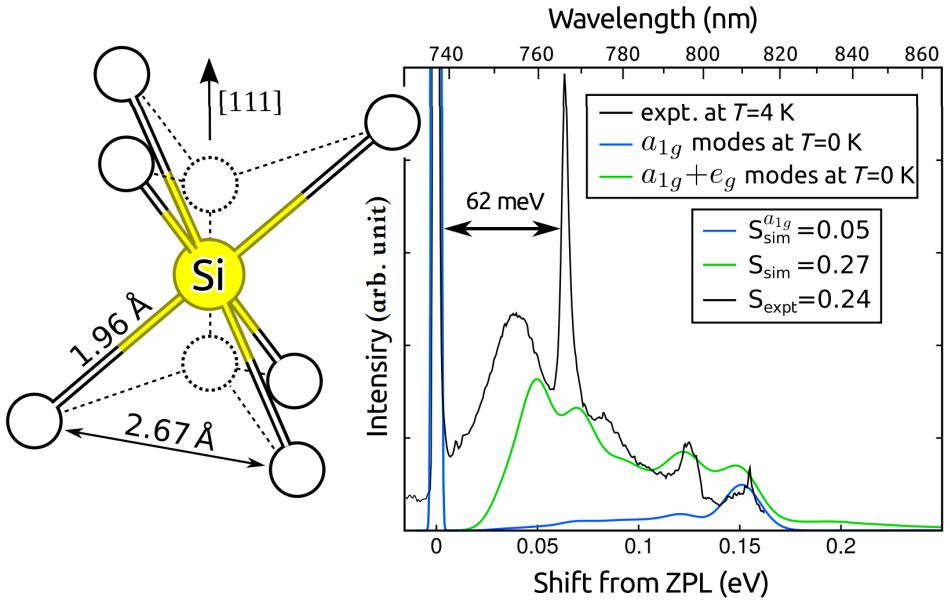

G. Thiering et al., *Phys. Rev. X* **8**, 021063 (2018).

Duschinsky rotation effect

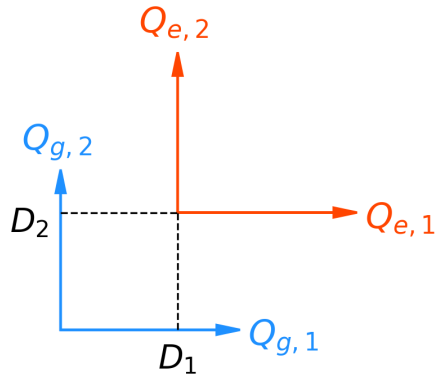

$$Q_{e,i} = Q_{g,i} + D_i$$

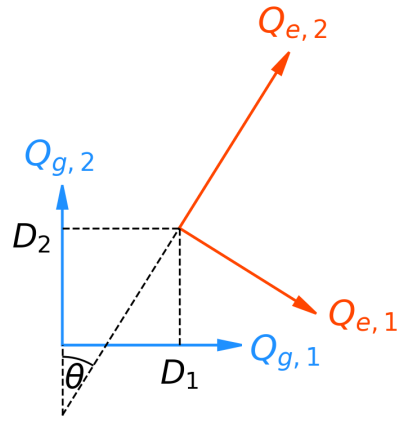

$$Q_{e,i} = \sum_j S_{ij}\, Q_{g,j} + D_i$$

Acknowledgement

Argonne NATIONAL LABORATORY

Dr. Gary Wolfowicz
Dr. Sean Sullivan
Dr. F. Joseph Heremans

U.S. DEPARTMENT OF ENERGY | Office of Science

MICCoM

NERSC National Energy Research Scientific Computing Center

THE UNIVERSITY OF CHICAGO | Office of Research and National Laboratories Research Computing Center